

# Effect of Hyperoxia, Hypercapnia, and Hypoxia on Cerebral Interstitial Oxygen Tension and Cerebral Blood Flow

Timothy Q. Duong,<sup>1\*</sup> Costantino Iadecola,<sup>2</sup> and Seong-Gi Kim<sup>1</sup>

**The assessment of cerebral interstitial oxygen tension (piO<sub>2</sub>) can provide valuable information regarding cerebrovascular physiology and brain function. Compartment-specific cerebral piO<sub>2</sub> was measured by <sup>19</sup>F NMR following the infusion of an oxygen-sensitive perfluorocarbon directly into the interstitial and ventricular space of the in vivo rat brain. <sup>19</sup>F T<sub>1</sub> measurements were made and cerebral piO<sub>2</sub> were obtained through in vitro calibrations. The effects of graded hyperoxia, hypercapnia, and hypoxia on piO<sub>2</sub> and cerebral blood flow (CBF) were investigated. Under normoxia (arterial pO<sub>2</sub> ~ 120 mm Hg), piO<sub>2</sub> was ~30 mm Hg and jugular venous pO<sub>2</sub> was ~50 mm Hg. During hyperoxia (arterial pO<sub>2</sub> = 90–300 mm Hg), piO<sub>2</sub> increased linearly with the arterial pO<sub>2</sub>. Following hypercapnia (arterial pCO<sub>2</sub> = 20–60 mm Hg), the piO<sub>2</sub> increased sigmoidally with increasing CBF. With hypoxia (arterial pO<sub>2</sub> = 30–40 mm Hg), CBF increased ~56% and piO<sub>2</sub> decreased to ~15 mm Hg. The hypoxia-induced CBF increase was effective to some extent in compensating for the reduced piO<sub>2</sub>. This methodology may prove useful for investigating cerebral piO<sub>2</sub> under pathologically or functionally altered conditions. Magn Reson Med 45:61–70, 2001. © 2001 Wiley-Liss, Inc.**

**Key words:** perfluorocarbon; pO<sub>2</sub>; BOLD; tissue oxygenation; hypocapnia; NMR; CBF; brain; tumor

The mammalian brain is an aerobic organ that depends on a continuous and adequate supply of oxygen to maintain its structural and functional integrity. Relatively moderate reduction in oxygen delivery can lead to severe brain dysfunction. If tissue oxygen delivery is sufficiently compromised, loss of consciousness can occur within seconds and irreversible neuronal damage within minutes (1). Thus, tissue oxygen tension in the brain is carefully regulated and may modulate in response to changes in neuronal activity. It can also be drastically perturbed in diseased states such as cerebral ischemia and brain tumors.

Oxygen in blood must cross the blood-brain barrier (BBB) into the interstitial space, and subsequently into the intracellular space to be utilized predominantly in the mitochondria. It has been proposed that the dissolved oxygen does not diffuse freely from the blood pool into the interstitial space because the BBB acts as a barrier to the passage of oxygen (2). If this were the case, a large gradient of O<sub>2</sub> concentration across the vascular-interstitial com-

partment would be expected. With the limited reports to date, this issue remains controversial (2), and the oxygen gradient across the vascular-interstitial space has not been established. For example, some laboratories have reported the mean tissue pO<sub>2</sub> (weighted average of all tissue compartments) to be close to, or below, venous pO<sub>2</sub> (3,4), while others reported the mean tissue pO<sub>2</sub> to fall in between the arterial and venous pO<sub>2</sub> (5). In addition, little is known regarding how the interstitial or tissue oxygen tension is modulated in response to changes in arterial oxygen tension and/or CBF. Thus, the ability to measure *compartment-specific* interstitial, arterial, and venous oxygen tension in the brain could potentially shed light on the underlying mechanism by which oxygen passes from the capillary across the BBB and into the brain tissue.

Tissue oxygen tension in general has been studied using a variety of techniques, including reflectance spectrophotometry (2,3), oxygen-sensitive microelectrodes (4,5), fluorescence quenching (6), optical and infrared probes (7), electron spin resonance oximetry (8), and the indicator-dilution technique (9). For example, in isolated mitochondrial preparations in vitro the critical oxygen tension necessary for mitochondria to function was determined to be as low as 1–2 mm Hg by using reflectance spectrophotometry (3). Based on these measurements, it has been speculated that the intracellular oxygen tension is on the same order of magnitude. Measurements using oxygen-sensitive electrodes have yielded valuable information regarding the distributions of tissue oxygen tension in the cerebral cortex. The mean *tissue* oxygen tension in the brain has been reported to be anywhere from 5 mm Hg (4) to 40 mm Hg (5). However, this technique can not be used to distinguish compartment-specific oxygen tension in the interstitial, intracellular, arterial, and venous blood spaces; thus, the measured pO<sub>2</sub> is a weighted average of all these compartments.

Alternatively, tissue oxygen tension can be measured using MR by exploiting the relaxation properties of <sup>19</sup>F-labelled perfluorocarbons (PFCs). The <sup>19</sup>F spin-lattice (R<sub>1</sub> ≡ 1/T<sub>1</sub>) and the spin-spin (R<sub>2</sub> ≡ 1/T<sub>2</sub>) relaxation rate constants of the perfluorocarbon are highly sensitive to oxygen tension because the paramagnetic molecular oxygen acts as an effective relaxation reagent on the <sup>19</sup>F perfluorocarbon. Furthermore, the <sup>19</sup>F R<sub>1</sub> and R<sub>2</sub> are linearly dependent on the dissolved oxygen concentration, making quantitative analysis relatively straightforward. There have been many previous investigations of tissue (10) and cerebrovascular oxygenation (11) using <sup>19</sup>F MR of perfluorocarbon emulsions following vascular infusion. In particular, tissue piO<sub>2</sub> measurements in animal models using intravenously administered PFCs have been reported in

<sup>1</sup>Department of Radiology, Center for Magnetic Resonance Research, University of Minnesota School of Medicine, Minneapolis, Minnesota.

<sup>2</sup>Department of Neurology, Laboratory of Cerebrovascular Biology and Stroke, University of Minnesota School of Medicine, Minneapolis, Minnesota. Grant sponsor: NIH; Grant numbers: RR08079; NS38295; NS10930; Grant sponsors: Keck Foundation; Whitaker Foundation.

\*Correspondence to: Timothy Q. Duong, Ph.D., Center for Magnetic Resonance Research, University of Minnesota School of Medicine, 2021 Sixth Street SE, Minneapolis, MN 55455. E-mail: duong@cmrr.umn.edu

Received 20 March 2000; revised 10 August 2000; accepted 11 August 2000.

liver (12,13), spleen (12,13), and brain with tumors (14,15). An alternative approach that uses direct injection of a perfluorocarbon into the organ of interest has been demonstrated previously in the eye (16).

In this study, we extended the  $^{19}\text{F}$  PFC applications to measure compartment-specific interstitial (as opposed to the weighted average tissue) oxygen tension in the rat brain in vivo under normal physiological conditions and following physiological perturbations. This application involved administering a compartment-specific,  $^{19}\text{F}$ -labelled, oxygen-sensitive PFC emulsion directly into the interstitial/ventricular space in the in vivo rat brain via intracerebro-ventricular infusion.  $^{19}\text{F}$  MR  $T_1$  measurements were made using volume-localized spectroscopy on the rat brain and the cerebral interstitial  $\text{pO}_2$  ( $\text{piO}_2$ ) was derived through in vitro calibration curves of  $^{19}\text{F}$   $1/T_1$  vs. dissolved oxygen partial pressure. In conjunction with blood-gas samplings and CBF measurements using the continuous arterial spin labeling technique (17–19), we applied this methodology to investigate: 1) the coupling between vascular and interstitial oxygen tension by modulating the inhaled oxygen concentration; and 2) the coupling between CBF and interstitial oxygen tension by modulating the inhaled carbon dioxide concentration. To the best of our knowledge, this study presents the first MR measurement of the compartment-specific, cerebral interstitial and ventricular  $\text{pO}_2$  in vivo in a serial, relatively noninvasive manner under hypercapnic, hyperoxic, and hypoxic conditions.

## METHODS

### In Vitro Calibration

The highly sensitive PFC, perfluoro-15-crown-5-ether (MW = 580.27 g/mole, Exflur Research Co., Round Rock, TX), was chosen as the marker for oxygen tension measurement because of its high sensitivity (12,20). With 20 equivalent  $^{19}\text{F}$  nuclides, this PFC gives rise to one single resonance (12,20) without the loss of signal sensitivity due to chemical-shift modulation. The PFC was emulsified in a mixture of 2% lecithin and 2% safflower oil, with an average emulsion size of  $\sim 200$  nm in diameter (40% v/v, Gateway Technology Inc., St. Louis, MO). In vitro calibrations relating  $R_1$  to  $\text{O}_2$  partial pressure were made using four or five different  $[\text{O}_2]$  bubbled into pure PFC emulsion samples for  $\sim 30$  min to equilibrium at  $37^\circ\text{C}$ . For the calibration at 9.4 T, the  $[\text{O}_2]$  used were 0, 21, 40, 60, and 100% with balance  $\text{N}_2$ . For the calibration at 4.7 T, the  $[\text{O}_2]$  used were 0, 21, 31, and 100%  $\text{O}_2$  with balance  $\text{N}_2$ . Two different samples were prepared for each gas condition at each magnetic field and two  $T_1$  measurements were made on each sample. The sample temperature was maintained at  $37.0 \pm 0.5^\circ\text{C}$  via a circulating warm water bath during the  $T_1$  measurements.  $^{19}\text{F}$  inversion-recovery measurements were made using 20 inversion delays (TI). Conversion of percent oxygen to units of mm Hg assumed that 100% oxygen is equal to 760 mm Hg.

### Animal Surgery

A total of 36 male Sprague Dawley rats (250–300 g) were anesthetized with 1% halothane (for the hyperoxia and

hypercapnia studies) or 1–2% isoflurane (for the hypoxia study) in a mixture of  $\text{O}_2$  and  $\text{N}_2$  gases. Following oral intubation, the animal was placed in a stereotaxic head frame (Stoelting, Wood Dale, IL) for intracerebro-ventricular (ICV) infusion of the PFC emulsion. Two small holes,  $\sim 1.0$  mm in diameter, were drilled in the skull to target the lateral ventricles at the coordinates of  $\pm 1.4$  mm lateral to the midline, 0.9 mm posterior from the bregma and 3.5 mm deep from the dura (21). Two stainless steel 30-gauge needles were stereotaxically placed into the lateral ventricles. A small volume ( $\sim 80$   $\mu\text{l}$ ) of the isotonic, pH-balanced emulsion was simultaneously infused into the two cerebral lateral ventricles via an infusion pump (Harvard Apparatus, South Natick, MA) over  $\sim 1$  hour. After the ICV infusion, a jugular vein and a femoral artery were catheterized with PE-50 tubing for blood-gas sampling and/or physiological monitoring. The end-tidal  $\text{CO}_2$  and the inspired gases ( $\text{O}_2$ ,  $\text{CO}_2$ , and  $\text{N}_2$ ) were continuously monitored using a capnometer (Detex-Ohmeda, Louisville, CO). The mean blood pressure and heart rate were monitored via the femoral artery by using a pressure transducer and a differential amplifier. The analog signals were digitized and recorded using the Biopac analog-to-digital converter and the Acknowledge software (Santa Barbara, CA). The animal's rectal temperature was monitored and maintained at  $37 \pm 1^\circ\text{C}$  throughout the experiments using a warm water bath, which was regulated via a feedback circuit.

Four groups of experiments were performed in which different  $\text{O}_2$  or  $\text{CO}_2$  concentrations with balance  $\text{N}_2$  were added to the inhaled gas. In group I (hyperoxia,  $N = 5$ , 1% halothane), seven to 10 different  $\text{O}_2$  concentrations ranging from 30 to 100% (typically: 30, 40, 50, 60, 70, 80, 90, and 100%  $\text{O}_2$ ) were added to the inhaled gas for each animal under  $\sim 1\%$  halothane. The arterial  $\text{pCO}_2$  (as determined by blood-gas and end-tidal  $\text{CO}_2$  sampling), and thus CBF, was maintained relatively constant. In group II (hypercapnia,  $N = 5$ , 1% halothane), seven to 10 different  $\text{CO}_2$  concentrations ranging from 0 to 7% (typically: 0, 0.5, 1, 2, 3, 4, 5, 6, and 7%  $\text{CO}_2$ ) were added to the inhaled gas for each animal under  $\sim 1\%$  halothane. The arterial  $\text{pO}_2$  ( $\text{paO}_2$ ) was maintained relatively constant. In group III (hypoxia,  $N = 16$ , 1% isoflurane), graded hypoxic hypoxia was achieved by systematically lowering the oxygen concentration of the inhaled gas in rats under  $\sim 1\%$  isoflurane. Five to seven different  $\text{O}_2$  concentrations ranging from 10 to 50% (typically, the  $[\text{O}_2]$  was decreased from 50, 28, 19, 14, 12, and 10% with balance  $\text{N}_2$  gas) were used in each animal. Four out of 16 rats in this group were used as control in which hypoxia was induced without ICV infusion. In group IV (hypoxia,  $N = 10$ , 2% isoflurane), similar graded hypoxic hypoxia was achieved in rats under  $\sim 2\%$  isoflurane. Four out of 10 rats in this group were used as a control in which hypoxia was induced without ICV infusion.

Blood-gas and MR measurements were made at least 15 min (typically 20 min) following each new gas condition. This duration was determined in some animals to be more than sufficient to ensure a steady state based on repeated blood-gas and  $^{19}\text{F}$   $T_1$  measurements. In all experimental groups, both  $^{19}\text{F}$   $T_1$  and  $^1\text{H}$  CBF measurements for each gas condition were made except in Group I, in which

only  $^{19}\text{F}$   $T_1$  measurements were made. Blood-gas samples ( $\sim 0.06$  cc each) were obtained from the femoral artery and jugular vein for each gas condition and analyzed by a blood-gas machine (Rapidlab Model 248, Chiron Diagnostics, East Walpole, MA). Hyperoxia (22), mild hypercapnia (22,23), and hypoxia (22) do not significantly alter cerebral metabolism. Similarly, hyperoxia does not significantly alter CBF if the arterial  $\text{pCO}_2$  is maintained relatively constant (22). At the end of most experiments, the animal was killed by an intravenous KCl (potassium chloride) overdose or by total hypoxia (inhaling 100%  $\text{N}_2$ ).  $^{19}\text{F}$   $T_1$ 's were measured from the time of death (indicated by the flattening of arterial blood pressure and/or end-tidal  $\text{CO}_2$ ) to  $\sim 15$  min after death.

### MR Experiments

All MR studies except the hyperoxia study were performed on a 9.4T/31cm (Magnex Scientific, Abingdon, UK) horizontal MRI scanner equipped with a 30-G/cm gradient (11.0 cm ID, 300- $\mu\text{s}$  rise time; Magnex Scientific). The hyperoxia study was performed on a 4.7T/40cm (Oxford Magnet, Oxford, UK) horizontal MRI scanner equipped with a 15-G/cm gradient (10.8 cm ID, 300- $\mu\text{s}$  rise time; in-house built). The MR scanners were independently driven by two essentially identical *Unity* INOVA consoles (Varian, Palo Alto, CA) and hardwares. After surgery, the animal was carefully secured in an in-house-built head holder with ear and bite bars to minimize head movement. A small surface coil of  $\sim 1.2$  cm in diameter, tunable to both  $^1\text{H}$  and  $^{19}\text{F}$  resonance frequencies, was positioned on top of the rat head. An image-guided voxel of  $\sim 10 \times 8 \times 8$  mm<sup>3</sup> was placed at the center of the brain. All of the MR parameters used on the two MR scanners were similar unless otherwise specified. Field homogeneity was optimized on the voxel by shimming to yield a  $^1\text{H}_2\text{O}$  spectral linewidth of  $\sim 20$  Hz at 9.4 T and  $\sim 15$  Hz at 4.7 T.  $^{19}\text{F}$  MR spectra were acquired using the volume-localized, double spin-echo, point-resolved spectroscopy (PRESS) sequence with an echo time of 22 msec at 9.4 T and 32 msec at 4.7 T. The three radiofrequency pulses in the PRESS sequence were 3-msec sinc pulses. A pair of crusher gradients (10 G/cm for 3 msec) was placed around each of the two  $180^\circ$  refocusing pulses to destroy residual transverse magnetization due to imperfect magnetization refocusing of the  $180^\circ$  pulses.

To measure  $\text{piO}_2$ ,  $^{19}\text{F}$  inversion-recovery measurements were made with seven variable inversion delays (0.19, 0.38, 0.75, 1.5, 3, 6, and 12 sec) and a delay of 5  $T_1$  between subsequent inversion experiments. Typically, 2–6 transients were accumulated for signal averaging in each  $^{19}\text{F}$   $T_1$  measurement. Four  $T_1$  measurements were made for each gas condition. Each  $T_1$  measurement took 3–5 min.

Quantitative CBF measurements were made on the same voxel by using the continuous arterial ( $^1\text{H}$ ) spin-labeling technique (18,19) in spectroscopy mode before or after the  $^{19}\text{F}$   $T_1$  measurements. Continuous arterial spin labeling (with 3-sec labeling time) employed a butterfly neck coil (0.5-cm diameter) placed at  $\sim 2$  cm posterior from the imaging coil. Typically, four sets of CBF measurements were made for each equilibrated gas condition, with each set consisting of eight pairs of labeled and nonlabeled

spectra. The sign of the frequency offset was switched for the control (nonlabeled) spectrum. Each set of CBF measurement took  $\sim 1$  min.

### Data Analysis

Inversion-recovery data were fitted to a three-parameter model using the non-linear least-square method. Determination of  $\text{piO}_2$  from the  $^{19}\text{F}$   $T_1$  measurements employed the standard calibration curves performed on the emulsion phantoms. The  $\text{O}_2$  partial pressure in mm Hg was converted to  $\text{O}_2$  concentration in mM based on the  $\text{O}_2$  solubility in hemoglobin and water (24). The latter was assumed to be representative of interstitial fluid and cerebrospinal fluid (CSF). Quantitative CBF values were calculated as described elsewhere (17–19) except that the small magnetization transfer effect from macromolecules was ignored. Statistical analysis employed a Student paired *t*-test, and a *P*-value of 0.05 was taken as the criterion for statistical significance unless otherwise specified. All reported values are in means  $\pm$  SD and all error bars in the graphs represent standard error of the mean (SEM) unless otherwise specified.

## RESULTS

### Calibration

From the linear least-squares analysis, the standard calibration curves for PFC  $^{19}\text{F}$   $R_1$  vs. dissolved oxygen partial pressure at the two magnetic fields (37°C) were:

$$R_1 \text{ (at 4.7 T)} = 0.362 + 0.00215 \text{ O}_2, R^2 = 0.999, \quad [1a]$$

and

$$R_1 \text{ (at 9.4 T)} = 0.445 + 0.00192 \text{ O}_2, R^2 = 0.998, \quad [1b]$$

where  $R_1$  is in  $\text{sec}^{-1}$  and  $\text{O}_2$  is the partial pressure of oxygen bubbled into the emulsion in mm Hg. The uncertainties (standard errors) of four repeated  $T_1$  measurements were typically  $\pm 0.01$  sec. The standard errors of the estimated slopes were  $2.5 \times 10^{-5}$  at 4.7 T and  $5.4 \times 10^{-5}$  at 9.4 T; those of the estimated intercepts were 0.01 at 4.7 T and 0.02 at 9.4 T.

### Physiology and Distribution

ICV infusion rate and volume were carefully adjusted to avoid seizure and central nervous system herniation. Rats tolerated the ICV infusion well and essentially all animals ( $> 90\%$ ) survived until they were euthanized. The animal's blood gas, end-tidal  $\text{CO}_2$ , arterial blood pressure, and heart rate were maintained within normal physiological ranges unless otherwise perturbed (pH = 7.35–7.47,  $\text{pCO}_2 = 32$ –42 mm Hg,  $\text{pO}_2 = 120$ –160 mm Hg, end-tidal  $\text{CO}_2 = 3.5$ –4.5% atmosphere, mean arterial blood pressure = 75–110 mm Hg, and heart rate = 340–380 bpm). The animal's rectal temperature was maintained at  $37.0 \pm 0.5^\circ\text{C}$  throughout the experiments.

To determine whether the PFC administered via the ICV infusion was reasonably distributed in the interstitial space in the brain,  $^{19}\text{F}$  MR spectra from multiple regions of

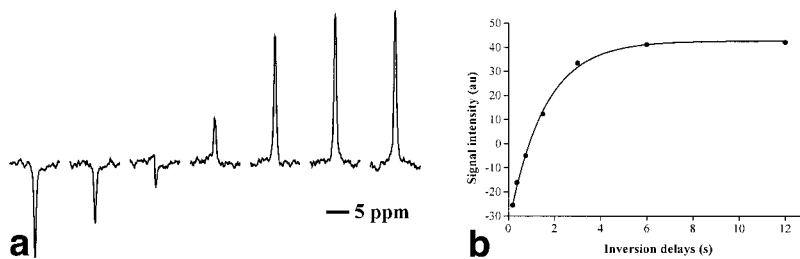


FIG. 1. **a:** A representative set of 9.4T<sup>19</sup>F inversion-recovery spectra obtained from a voxel ( $10 \times 8 \times 8 \text{ mm}^3$ ) including essentially the entire brain. The  $T_1$  measurement took  $\sim 3$  min. The FWHM of each spectrum was  $\sim 100$  Hz and a line broadening of 100 Hz was used. **b:** An inversion-recovery plot of the spectra. The solid curve is the three-parameter  $T_1$  fit to the data, yielding a  $T_1$  of 1.65 sec. The arterial and venous blood gases of the animal immediately after this  $T_1$  was measured were 252 and 67 mm Hg, respectively.

the brain were acquired starting at  $\sim 1$  hr and continuing up to  $\sim 6$  hours after the end of the ICV infusion in some animals. The regions of equal volume ( $\sim 2 \times 2 \times 4 \text{ mm}^3$ ) selected for the MR acquisition were the forepaw primary somatosensory cortex, the caudate putamen, and the lateral ventricle. Approximately 1 hr after the ICV infusion, <sup>19</sup>F MR signals were clearly detectable in the ventricular voxel with little or no signals from the other two voxels. As time evolved, the <sup>19</sup>F MR signals became detectable in other regions in addition to the ventricular voxel. The highest signal amplitude per volume remained localized around the lateral ventricles. At  $\sim 4$  hours, the voxel signal amplitudes in the caudate putamen and the somatosensory cortex were  $\sim 10$ – $30\%$  that of the ventricular voxel per volume basis and did not appear to change much after  $\sim 4$  hr. This was most likely due to the relatively large interstitial and CSF space in and around the lateral ventricular spaces. Given the small size of the PFC emulsion particles of  $\sim 200$  nm, they should have little difficulty in distributing to the cerebral interstitial spaces, which are on the order of a few microns. However, sufficient time must be allowed for the distribution because CSF circulation is relatively slow. Based on these results and previous experience (21),  $\sim 4$  hr was necessary for the PFC to be reasonably distributed. Therefore, <sup>19</sup>F  $T_1$  measurements to obtain  $\text{piO}_2$  were made starting at least 4 hr after the termination of the ICV infusion. Due to the presence of significant signal contamination from the ventricular spaces, the term “interstitial” space is used herein to collectively refer to include both the interstitial and ventricular spaces.

Figure 1a shows a representative set of <sup>19</sup>F volume-localized, inversion-recovery spectra at 9.4 T (spectra at 4.7 T were of comparable quality). The corresponding inversion-recovery plot is shown in Fig. 1b. The three-parameter  $T_1$  fitting yielded a  $T_1$  value of 1.65 sec, corresponding to an interstitial/ventricular  $\text{pO}_2$  of  $\sim 84$  mm Hg (Eq. [1]). The uncertainties (standard errors) in the in vivo  $T_1$  values obtained from a single measurements and from four repeated measurements were typically  $\pm 0.01$  and  $\pm 0.015$  sec, respectively. The arterial and venous blood gases of the animal immediately after this  $T_1$  measurement were  $\sim 252$  and  $\sim 67$  mm Hg, respectively. The errors associated with the repeated blood-gas  $\text{pO}_2$  measurements were estimated to be on the order of 5–10% ( $\pm 10$  mm Hg at  $\sim 200$  mm Hg and  $\pm 5$  mm Hg at  $\sim 50$  mm Hg). Note that the venous blood gases referred to in this work were obtained from the jugular vein, which is slightly contaminated with some blood draining from the face and head in rats. However, for systemic physiological modulations such as hyperoxia, hypercapnia, and hypoxia, jugular ve-

nous blood-gas values are reasonably representative of the cerebral venous blood gas values (25).

At the end of most experiments, the animals were sacrificed via intravenous KCl overdose. The average  $T_1$  within  $\sim 15$  min postmortem was  $2.17 \pm 0.05$  sec ( $N = 15$ ) at 9.4 T, slightly lower than the in vitro value of 2.25 sec at 0 mm Hg [ $\text{O}_2$ ]. This is likely due to the slight decrease in brain temperature and/or residual tissue oxygenation after death. Rectal temperature dropped by  $< 1^\circ\text{C}$  within 20 min postmortem, and brain temperature was likely to decrease slightly more. The presence of residual tissue oxygen tension was confirmed by comparing the postmortem  $T_1$  values in rats killed by KCl overdose and by total hypoxia (inhaling 100%  $\text{N}_2$ ). The  $T_1$  from total hypoxia, which presumably left negligible residual tissue  $\text{pO}_2$ , yielded a larger  $T_1$  ( $2.20 \pm 0.05$  sec,  $N = 5$ ), closer to the in vitro calibration value at 0 mm Hg [ $\text{O}_2$ ].

In a separate set of experiments in which <sup>19</sup>F  $T_1$  was measured using 64 logarithmic-spaced, inversion-recovery delays (with 8–10 transients accumulated for signal averaging), bi-exponential characteristics were not detected in live animals. Similarly, bi-exponential characteristics were also not detected postmortem (data not shown). Thus, all subsequent  $T_1$  measurements were made with 7 inversion delays to obtain a mono-exponential  $T_1$ .

### Hyperoxia (Group I)

Cerebral interstitial, arterial, and venous blood-gas oxygen tensions were measured at different inhaled oxygen concentrations. Figure 2 shows the MR-derived  $\text{piO}_2$  in brain and the jugular vein blood-gas  $\text{pO}_2$  ( $\text{pvO}_2$ ) as a function of arterial blood-gas  $\text{pO}_2$  ( $\text{paO}_2$ ). The  $\text{piO}_2$  increased roughly linearly with  $\text{paO}_2$  (from 90–300 mm Hg). The  $\text{piO}_2$  rises from a value below the  $\text{pvO}_2$  to a value above the  $\text{pvO}_2$ , with the intercept between the interstitial and venous  $\text{pO}_2$  curves at  $\sim 180$  mm Hg  $\text{paO}_2$ . At normal physiological  $\text{paO}_2$  ( $\sim 120$  mm Hg) and CBF, the cerebral  $\text{piO}_2$  was  $\sim 30$  mm Hg, significantly lower than the  $\text{paO}_2$  and slightly lower than the  $\text{pvO}_2$  ( $\sim 50$  mm Hg). The  $\text{pvO}_2$  increased over a small range (50–70 mm Hg) as the  $\text{paO}_2$  was modulated from 90–300 mm Hg. The average arterial  $\text{pCO}_2$  ( $\text{paCO}_2$ ) for all animals in the hyperoxia experiments was  $36 \pm 8$  mm Hg ( $N = 5$ ).

### Hypercapnia (Group II)

The cerebral interstitial, arterial, and venous oxygen tensions and CBF were measured at different inhaled carbon dioxide concentrations. Figure 3a shows the MR-derived

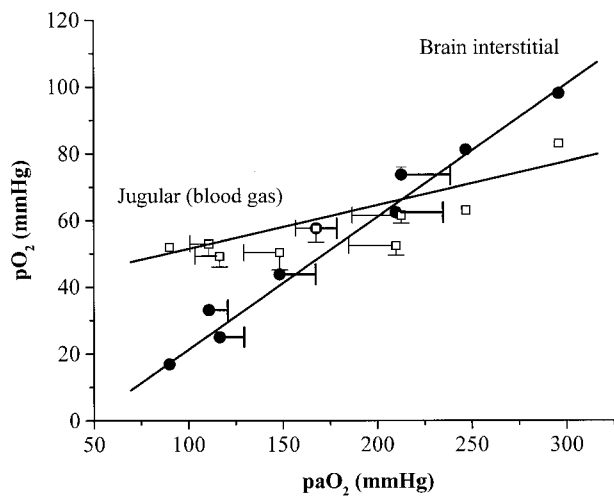


FIG. 2. In vivo interstitial and venous oxygen tension as a function of arterial oxygen tension. There is a positive correlation between the cerebral interstitial and arterial oxygen tension (circles). The intercept between the interstitial and venous  $pO_2$  curves is at  $\sim 180$  mm Hg  $paO_2$ . All error bars are SEMs. The lowest  $paO_2$  data points do not have error bars. Some error bars are too small and thus not visible.

CBF as a function of  $paCO_2$ . A rough sigmoidal shape was observed, consistent with the well known hypercapnia-induced CBF increase reported in the literature (26,27). The average  $paO_2$  for all animals in the hypercapnia experiments was  $148 \pm 16$  mm Hg ( $N = 5$ ).

Figure 3b shows the MR-derived  $piO_2$  as a function of CBF. The curve also appears to be sigmoidal in shape. At a normal physiological CBF of  $\sim 1$  ml/g/min, the average  $piO_2$  measured in the hypercapnia study was consistent with that measured in the hyperoxia study, which were performed on a different group of animals and at a different magnetic field (same anesthetics). The  $piO_2$  increases approximately linearly with CBF over the physiological range of  $\sim 1.0$ – $2.0$  ml/g/min and appears to reach a plateau at  $\sim 2.3$  ml/g/min. In the linear portion of the curve (CBF =  $1$ – $2$  ml/g/min),  $\sim 100\%$  increase in CBF resulted  $\sim 50\%$  increase in  $piO_2$ . Figure 3b also shows that the  $pVO_2$  increased over a small range (65–75 mm Hg) as a function of CBF.

#### Hypoxia (Groups III and IV)

Graded hypoxia was studied in a total of 11 ICV-infused rats under  $\sim 1\%$  isoflurane anesthesia (Group III). At the start of the experiments with the animals inhaling  $\sim 50\%$  oxygen, the average  $paO_2$  was  $198 \pm 13$  mm Hg and  $pVO_2$  was  $67 \pm 9$  mm Hg. Hypoxic hypoxia was induced by systematically lowering the oxygen concentration of the inhaled gas without changing the ventilator settings. The lowest  $paO_2$  typically achieved was  $\sim 30$ – $40$  mm Hg, resulting from inhaling 10–12% oxygen. Figure 4a shows the group-averaged CBF and  $piO_2$  as a function of  $paO_2$  under 1% isoflurane for 9 of the 11 rats. No hypoxia-induced CBF increases were observed in two of the animals and they were not further analyzed. The baseline non-hypoxic CBF value was  $0.87 \pm 0.27$  ml/g/min. CBF

increased exponentially as the  $paO_2$  dropped below  $\sim 60$  mm Hg. Under hypoxic conditions with  $\sim 30$ – $40$  mm Hg  $paO_2$ , the CBF increased by  $\sim 56\%$  relative to normoxia (from  $0.87 \pm 0.27$  to  $1.35 \pm 0.43$  ml/g/min), consistent with the average  $\sim 54\%$  hypoxia-induced CBF increases previously reported in the rat brain (28). In contrast to the normoxic and hyperoxic conditions, the  $piO_2$  ( $\sim 15$  mm Hg) was markedly lower than the  $pVO_2$  ( $29 \pm 7$  mm Hg) under hypoxic conditions with  $\sim 30$ – $40$  mm Hg  $paO_2$ . The  $piO_2$  consistently decreased with decreasing  $paO_2$  despite the hypoxia-induced CBF increase.

The arterial and venous blood-gas pH under hypoxia (30–40 mm Hg  $paO_2$ ) were not statistically different from normoxia. The mean arterial blood pressures also remained relatively constant at  $\sim 100$  mm Hg. On the other hand, the arterial blood-gas  $pCO_2$  decreased from  $35 \pm 2$  (normoxia) to  $29 \pm 4$  mm Hg ( $P = 0.002$ ), suggesting that the animals became hypocapnic, likely resulting from the hypoxia-induced CBF increase. The heart rates increased from  $\sim 380$  bpm at normoxia to  $\sim 450$  bpm at  $paO_2$  of

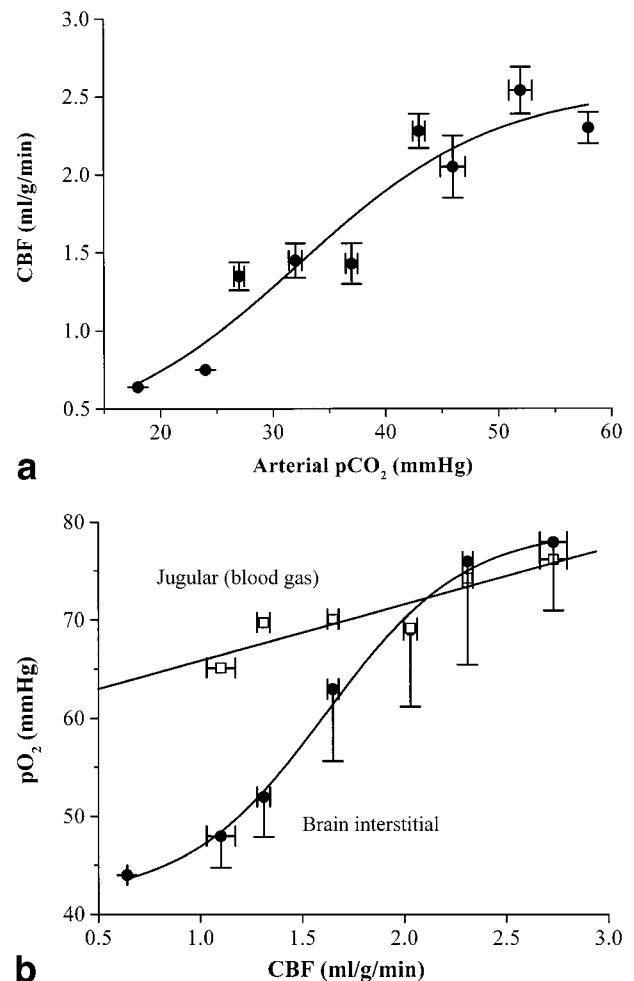


FIG. 3. **a:** CBF as a function of arterial blood-gas  $pCO_2$ . The CBF- $pCO_2$  relationship appears sinusoidal. **b:** Cerebral interstitial and venous  $pO_2$  as a function of CBF. The relationship between interstitial oxygen tension and CBF also appears to be sigmoidal. All error bars are SEMs. The lowest CBF data point does not have an error bar.

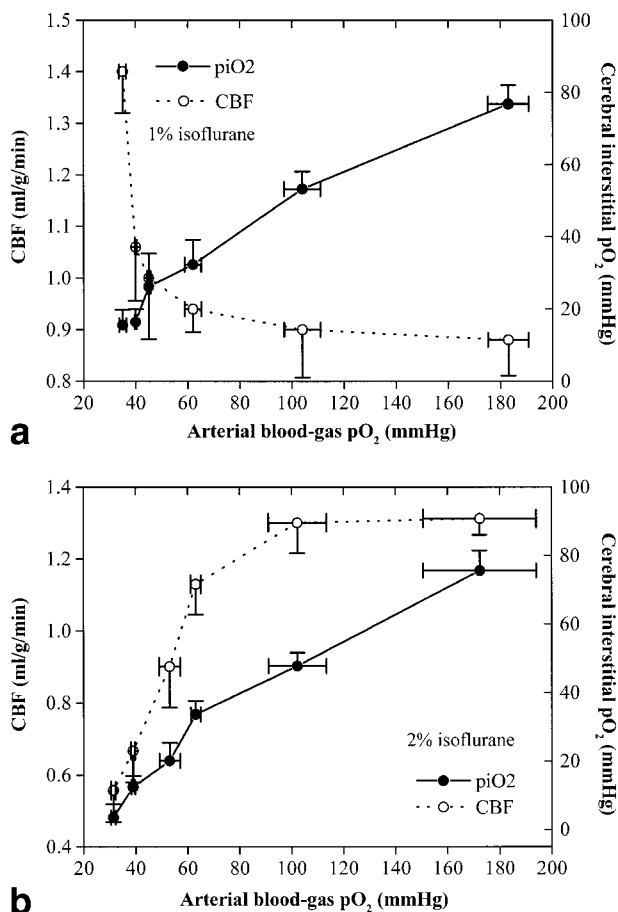


FIG. 4. CBF and  $piO_2$  as a function of arterial blood-gas  $pO_2$  under (a)  $\sim 1.0\%$  and (b)  $\sim 2\%$  isoflurane during hypoxia. Under  $\sim 1\%$  isoflurane, CBF increased exponentially as  $paO_2$  decreased below  $\sim 60$  mm Hg. Under  $\sim 2\%$  isoflurane, hypoxia-induced CBF increases were not observed; rather, CBF monotonically decreased with decreasing  $paO_2$  starting at  $\sim 60$  mm Hg  $paO_2$ . The interstitial  $pO_2$  under both anesthesia levels decreased monotonically following graded hypoxia (see also Fig. 5).

30–40 mm Hg. These observations are in good agreement with those reported previously (28–30).

It is possible that the combined effect of ICV infusion might have compromised the hypoxia-induced CBF response to some extent. Thus, as a control, hypoxia was also induced in rats under identical conditions but without ICV infusion. The hypoxia-induced CBF increase was  $\sim 50\%$  when the  $paO_2$  was reduced to  $34 \pm 4$  mm Hg ( $N = 4$ ). These data indicate that ICV per se did not significantly alter the hypoxia-induced CBF response under these conditions.

To investigate the anesthetic effect on the cerebrovascular response to hypoxia, similar graded hypoxia experiments were performed on six rats under 2% isoflurane (Group IV). At the start of the experiments with the animals inhaling  $\sim 50\%$  oxygen, the average arterial and venous  $pO_2$  were  $\sim 210$  and  $\sim 70$  mm Hg, respectively. None of the rats under 2% isoflurane exhibited hypoxia-induced CBF increases (Fig. 4b). Rather, CBF monotonically decreased with decreasing  $paO_2$  starting at  $\sim 60$  mm Hg  $paO_2$ .

The  $piO_2$  also decreased monotonically as a function of  $paO_2$ . The arterial and venous blood-gas pH under hypoxia (30–40 mm Hg  $paO_2$ ) were not statistically different from that under normoxia, while heart rate increased slightly from 380 to 440 bpm, consistent with hypoxia under  $\sim 1\%$  isoflurane. Unlike hypoxia under  $\sim 1\%$  isoflurane, there was a significant drop in mean arterial blood pressure from  $\sim 80$  to  $\sim 40$  mm Hg under hypoxia with  $\sim 2\%$  isoflurane. The end-tidal  $CO_2$  was 3.5–4.5% before hypoxia and it gradually decreased starting at  $\sim 50$  mm Hg  $paO_2$  and reached  $\sim 1.5\%$  at 30–40 mm Hg  $paO_2$ . These data suggested that oxygen metabolism in hypoxic rats under 2% isoflurane was markedly reduced. To exclude the possible effects of ICV infusion per se on the hypoxic response, similar control experiments were performed in which hypoxia was induced in rats under 2% isoflurane without ICV infusion. No CBF increases associated with hypoxia were observed (data not shown,  $N = 4$ ), suggesting that the cerebrovascular regulation under hypoxia was impaired under heavy anesthesia and that the absence of hypoxia-induced CBF increase was unlikely to be a direct consequence of ICV infusion per se.

In blood, oxygen partial pressure (mm Hg) is not a linear function of oxygen concentration (mM) because hemoglobin binds oxygen in a cooperative fashion, while in the interstitial fluid oxygen partial pressure is a linear function of oxygen concentration. Therefore, it is informative to re-plot arterial and interstitial  $pO_2$  of Fig. 4 in units of mM oxygen concentration (Fig. 5). At arterial  $pO_2$  of  $\sim 120$  mm Hg, the interstitial  $[O_2]$  is  $\sim 0.5$  mM. Under 1% isoflurane, there is a clear plateau in interstitial oxygen concentration at  $\sim 0.2$  mM ( $\sim 15$  mm Hg) as the  $paO_2$  dropped below  $\sim 60$  mm Hg, suggesting that the  $piO_2$  is compensated to some extent. Based on these curves, the critical  $piO_2$  was estimated to be  $< 15$  mm Hg or  $< 0.20$  mM. On the other hand, the interstitial oxygen concentration under 2% isoflurane decreased slightly faster and to a lower value than that under 1% isoflurane. This is

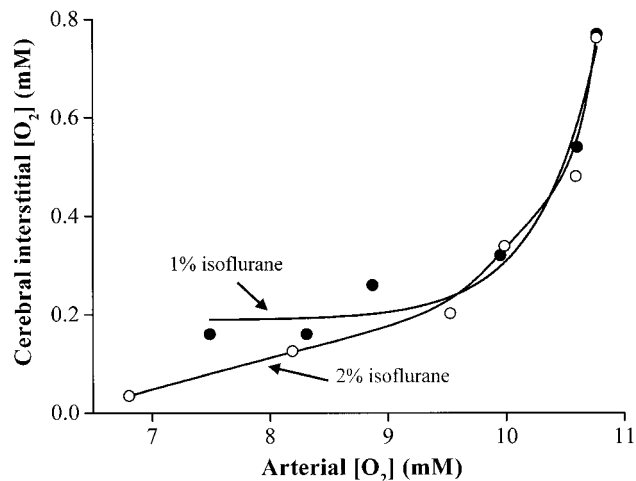


FIG. 5. Interstitial  $O_2$  concentration (in mM) as a function of arterial blood-gas  $O_2$  concentration. The interstitial oxygen concentrations markedly decreased following graded hypoxia. The interstitial  $O_2$  leveled off under 1% isoflurane but not under 2% isoflurane. The critical  $piO_2$  was estimated to be  $< 0.20$  mM or  $< 15$  mm Hg.

likely to be related to the absence of hypoxia-induced CBF increase under 2% isoflurane. It should be noted that the  $[O_2]$  estimates were obtained without taking into account the effect of  $pCO_2$ , pH, and other factors on the hemoglobin  $O_2$ -dissociation curve. Therefore, the reported  $[O_2]$  should be considered to be rough estimates under hypoxic conditions.

## DISCUSSION

### Assessment of the ICV Perfluorocarbon Infusion

PFC emulsions are known to be excellent blood substitutes, and their biocompatibility in general has been extensively reviewed (24). Some PFCs have been approved for human use and many others are currently undergoing clinical trials (24). Specifically, no short-term ill effects have been observed associated with the intravenous use of perfluoro-15-crown-5-ether emulsion in mice with tumor (12) and normal rats (20), though a study reported some ill effects in nude mice implanted with human glioma (31). In the application presented in this work, the emulsion was administered directly into the interstitial/ventricular space. The ICV infusion volume was small relative to the interstitial and CSF volume (estimated to be  $\sim 1cc$ , as extrapolated from human data). In conjunction with the slow infusion rate, the adverse effect of a possible increase in cranial pressure was minimized. The small volume infused unfortunately made  $^{19}F$  imaging impractical. Following the ICV infusion, no short-term ill effects were observed, as indicated by the normal blood gas, mean blood pressure, heart rate, and survival rate. Furthermore, the animals were responsive to a wide range of physiological perturbations, such as hypercapnia and hypoxia. However, the long-term effects of the ICV infusion of the emulsion remain to be investigated.

There are two main drawbacks associated with this ICV approach in measuring  $piO_2$ . First, there was some tissue damage around the injection sites. However, the area of damage is small compared to the voxel size, so measurements reflect predominantly intact brain tissue. Second, the PFC distribution was weighted toward the cerebral ventricles and subarachnoid spaces per volume basis. However, the cerebral lateral ventricular volume was small compared to the interstitial/ventricular space of the whole brain voxel. A smaller, compartment-specific oxygen-sensitive marker might be more readily distributed in the interstitial space, potentially resulting in less weighting toward the large CSF spaces. Nevertheless, the oxygen tension in the cerebral ventricles had been estimated to be similar to that in the interstitial space using oxygen-sensitive electrode technique (32). An interesting alternative to PFC emulsion in this context is to use its non-emulsified form (16). While the intravascular administration of the non-emulsified PFC is known to cause vascular embolism, the ICV infusion of the non-emulsified PFC does not suffer such a drawback. Since the non-emulsified PFC is biologically inert and rarely toxic, its potential application in this context should be evaluated as it may yield better signal sensitivity per unit volume and more uniform distribution based on its size.

### Accuracy and Precision of the $pO_2$ Measurement

The accuracy of the estimated  $piO_2$  is predominantly dependent on how accurately the  $^{19}F T_1$  is measured. The  $T_1$  uncertainty in vivo was typically  $\pm 0.015$  sec (SEM) for the four repeated measurements. Based on the uncertainties of the estimated slope and intercept of Eq. [1], the uncertainties of the estimated in vivo  $pO_2$  were  $\sim 4\%$  ( $= 2$  mm Hg) at high (50 mm Hg) and  $\sim 9\%$  ( $= 1.35$  mm Hg) at low (15 mm Hg)  $piO_2$ . Another potential source of inaccuracy was temperature fluctuation and its effect on the  $T_1$  value.  $^{19}F$  PFC  $T_1$  has been shown to be temperature dependent (12). However, the in vitro and in vivo studies herein were performed at  $37.0 \pm 0.5^\circ C$ ; thus, the  $T_1$  error arising from temperature variation was unlikely to be significant. Based on Dardzinski and Sotak's (12) temperature calibration at 2 T (12), a  $piO_2$  error of  $< 4$  mm Hg is expected for the maximum  $\sim 1^\circ C$  drops in temperature postmortem.

The precision of the  $piO_2$  measurement is dependent on how well the in vitro calibration reflects the in vivo  $piO_2$ . CSF is predominantly made up of water with low substrate concentrations, and paramagnetic molecular oxygen is the predominant relaxation reagent on the  $^{19}F$  PFC (12,20). Therefore, oxygen tension calibration performed in water instead of artificial CSF is unlikely to significantly compromise the precision of the in vivo  $piO_2$  measurement. The slightly smaller postmortem  $T_1$  following KCl overdose compared to the 0-mm Hg  $[O_2]$  in vitro is most likely due to the residual tissue oxygen and/or brain temperature drop postmortem.

### Hyperoxia

In principle, the oxygen tension in the interstitial space is dependent on oxygen consumption and delivery. The latter is further dependent on the arterial blood oxygen capacity, CBF, and capillary permeability to oxygen. It is well established that oxygen consumption and CBF remain relatively unchanged during hyperoxia (22). The capillary permeability remains relatively constant (it may decrease slightly under acute and/or prolonged hyperoxia) (22). Thus, the measured  $piO_2$  was exclusively dependent on the arterial oxygen capacity, which was the only modulated parameter in the hyperoxia study. At physiological  $paO_2$  ( $paO_2 \sim 120$  mm Hg), the average cerebral  $piO_2$  was  $\sim 30$  mm Hg. As of yet, there are no data in the literature on the compartment-specific cerebral  $piO_2$  with which to compare our values. A wide range of mean tissue oxygen tensions from 5 mm Hg (4), 25 mm Hg (33), to 40 mm Hg (5) has been reported by using the oxygen-sensitive electrode technique. However, this technique reported a convolution of oxygen tension in the vascular, interstitial, and intracellular spaces, and thus can not be directly compared with our data. Nevertheless, our data are consistent with these electrode measurements, the values of which are expected to be lower due to the weighted contribution from the low- $pO_2$  intracellular compartment.

A roughly linear relationship between the  $piO_2$  and  $paO_2$  was observed. This is consistent with the notion that oxygen passage across the BBB is predominantly passive. In other words, the oxygen passage across the BBB is likely to be driven by the oxygen partial pressure gradient and

not by active or facilitated transport. If active and/or facilitated transport were present, a saturation effect at high  $paO_2$  would be expected. At normal physiological  $paO_2$ , the  $piO_2$  was slightly lower than  $pVO_2$ , suggesting that oxygen delivery was in delicate equilibrium with oxygen consumption under basal neural activity. At high  $paO_2$ , the  $piO_2$  was slightly higher than the  $pVO_2$ . This is not unexpected since the measured  $piO_2$  was an *average* value representing the interstitial spaces in exchange with the arterial and venous ends of the capillary beds. Thus,  $piO_2$  could be higher than the  $pVO_2$  if the oxygen supply exceeded the oxygen demand. At low  $paO_2$ , on the other hand, the  $piO_2$  was slightly lower than the  $pVO_2$ . This appeared to be the effect of  $O_2$  consumption, which decreased the  $piO_2$ . These data, however, did not suggest that the oxygen supply was limiting, only that  $O_2$  consumption exerted an observable effect on the interstitial oxygen pool, leaving it at a lower equilibrium value.

Absolute  $O_2$  concentrations in units of mM in the interstitial, arterial, and venous compartments were estimated based on the  $O_2$ -carrying capacities of hemoglobin and interstitial fluid. The  $O_2$ -carrying capacity of hemoglobin is ~20% volume at 150 mm Hg and ~18% volume at 50 mm Hg. The  $O_2$ -carrying capacity of water is ~0.4% at 30 mm Hg (~2% volume at 150 mm Hg) (24). Based on these data, the  $O_2$  concentration (in % volume or mM) in the ventricular/interstitial spaces under normal physiological conditions was estimated to be ~50 and ~45 times less than that in the arterial and venous blood, respectively. In marked contrast, the  $O_2$  partial pressure in the interstitial space was only ~3 times lower than that in the arterial blood and ~1.5 lower than that in the venous blood under normal physiological conditions.

### Hypercapnia

The relationship between  $piO_2$  and CBF was roughly linear for the CBF values of 1–2 ml/g/min. At this range, a 100% increase in CBF resulted in ~50% increase in oxygen delivery to the interstitial space, suggesting that the decreased transit time resulting from increased CBF had a significant effect on the oxygen passage across the BBB. This notion is consistent with the observation that at high CBF (i.e., > 2.3 ml/g/min) the effect of the shortened capillary transit time on the oxygen extraction fraction appeared to become more important, resulting in the  $piO_2$  plateau as the CBF continued to increase. Additionally, it is also possible that vessel dilation induced by  $CO_2$  might be reaching, or is already at, maximum despite further CBF increase, resulting in the  $piO_2$  plateau.

Interstitial oxygen tension measurement associated with hypercapnia is of particular interest in the context of oxygen delivery to the interstitial space following increased neural activity. It has been well established that there is a direct coupling between regional CBF and neural activity (34). The degree of coupling between neural activity and oxidative metabolism associated with increased neuronal activity, however, remains controversial (35,36). Based on the hypercapnia data in which the  $piO_2$  increase was half of the hypercapnia-induced CBF increase, ~25%  $piO_2$  increase is expected for the typical ~50% (35,37) stimulus-induced CBF increase in the human visual cortex. This

$piO_2$  increase is substantial. Furthermore, the stimulus-induced increase in oxygen consumption could potentially increase the oxygen pressure gradient, resulting in an increased delivery of oxygen to the interstitial space. Measurement of cerebral  $piO_2$  associated with neural stimulation is expected to yield valuable insights into the changes in oxygen delivery and metabolism associated with brain functions.

### Hypoxia

Cerebral hypoxia is a much studied phenomenon because it is associated with many clinical conditions, ranging from pulmonary and circulatory disorders to reduced inspired oxygen tension, such as from high altitude exposure and entrapment in a confined space (29). It is also relevant to tumor radiotherapy, as hypoxic tumor tissue is believed to be less susceptible to radiation treatment (38). The most prominent physiological response to cerebral hypoxia is a global increase in CBF. Unlike the hyperoxia and hypercapnia studies in which either  $O_2$  or CBF was independently modulated, both  $O_2$  and CBF changed simultaneously under hypoxia. Under hypoxic conditions, CBF increased exponentially, starting at ~60 mm Hg  $paO_2$ . The average CBF increase was ~55% when the  $paO_2$  reached 30–40 mm Hg under 1% isoflurane. The degree of CBF increase is dependent on the severity of the hypoxia, species, tissue types, basal CBF, and the level and type of anesthesia (1). Hypoxia-induced CBF increases had been reported to range from 25~90% in awake rats exposed to 10% oxygen (28), ~80% in choral-hydrate anesthetized rats with a  $paO_2$  of 49 mm Hg (39), to 200–250% in halothane-anesthetized sheep with a  $paO_2$  of 40 mm Hg (40). Following graded hypoxia under 1% isoflurane, the interstitial  $[O_2]$  decreased monotonically and then leveled off as the  $paO_2$  was further reduced from 60 to 30 mm Hg, suggesting that the hypoxia-induced CBF increase was effective to some extent in compensating for the reduced  $paO_2$ . The critical  $piO_2$  was estimated to be <15 mm Hg or <0.20 mM. Since the  $piO_2$  was ~15 mm Hg under hypoxia (1% isoflurane) with increased CBF compensation and the fractional increase of  $piO_2$  was half that of CBF, the  $piO_2$  under hypoxia without CBF compensation was estimated to be ~10 mm Hg.

It is interesting that the interstitial oxygen partial pressure in mm Hg decreased monotonically with graded hypoxia, while the interstitial oxygen concentration in mM leveled off. This is not at all surprising because the oxygen unloading of hemoglobin is particularly effective in the hypoxic  $paO_2$  range of 30–40 mm Hg. In this  $paO_2$  range, the rapidly changing portion of the sigmoidal saturation curve yields a disproportionately large unloading of oxygen concentration for a small change in arterial oxygen partial pressure. Therefore, plotting the interstitial oxygen concentration against the arterial oxygen concentration yielded a leveling-off effect, while plotting  $piO_2$  against  $paO_2$  in a partial pressure unit shows a monotonic decrease.

### Anesthesia Dependence

With regard to the effect of different types of anesthesia on the interstitial oxygen tension, a difference in  $piO_2$  under

isoflurane and halothane anesthesia was observed. For example, at 100 mm Hg  $p\text{aO}_2$  the  $p\text{iO}_2$  was  $\sim 25$  mm Hg under halothane anesthesia and  $\sim 50$  mm Hg under isoflurane anesthesia. Though it is possible that small systematic errors could arise from experiments performed at different fields and on different rat groups, these data suggest that anesthesia has a significant effect on the cerebrovascular physiology and oxygen delivery to the tissue. The fact that the cerebral  $p\text{iO}_2$  under isoflurane was higher than that under halothane is consistent with our observations that CBF (and thus  $p\text{iO}_2$ ) is higher under isoflurane than under halothane (which is in turn higher than under  $\alpha$ -chloralose). It is possible that different types of anesthesia have different effects on the CBF regulation, resulting in a different amount of  $p\text{O}_2$  delivered to the interstitial space. It is also possible that different types of anesthesia have different effects on the basal  $\text{O}_2$  metabolism and thus affect the  $p\text{iO}_2$ . Furthermore,  $p\text{iO}_2$  measurements under different anesthesia in the same animals should be helpful in evaluating the effect of anesthesia on oxygen delivery across the BBB and into the brain tissue.

With regard to the effect of different levels of the same anesthesia (1% vs. 2% isoflurane), no significant difference in  $p\text{iO}_2$  was observed under non-hypoxic conditions. However, the cerebrovascular response to hypoxia at a high dose (2%) of isoflurane was impaired, as indicated by the absence of the hypoxia-induced CBF increase. This could be associated with the dramatic drop in mean arterial blood pressure. It would be interesting to investigate whether the hypoxia-induced CBF response is present under  $\sim 2\%$  isoflurane if the mean arterial blood pressure were actively maintained within normal physiological ranges (i.e., by administration of an intravascular hyperosmotic agent). Since the end-tidal  $\text{CO}_2$  was also reduced under heavy anesthesia, these data indicated that cerebral metabolism associated with hypoxia was also markedly reduced. Without a hypoxia-induced CBF increase, it is therefore not surprising that the  $p\text{iO}_2$  in rats under 2% isoflurane was not compensated following graded hypoxia. These results could have strong implications in the clinical settings in which hypoxia occurs in anesthetized patients.

## CONCLUSIONS

We demonstrated that the compartment-specific interstitial/ventricular oxygen tension in the rat brain could be measured in a serial and relatively noninvasive manner using MR. We further employed this methodology, in conjunction with CBF and blood-gas measurements, to investigate the couplings among CBF, vascular, and interstitial oxygen tension under hyperoxic, hypercapnic, and hypoxic conditions. This methodology could prove useful in investigating the dynamic coupling between CBF and interstitial oxygen tension changes associated with increased neuronal activity and cerebral pathophysiology in animal models.

## ACKNOWLEDGMENTS

S.G.K. is a NAMI Olmsted County Investigator. A large part of this work was done with NIH postdoctoral support to T.Q.D. (NS10930).

## REFERENCES

- Siesjo B. Brain energy metabolism. New York: Wiley; 1978. p 398–446.
- Chance B. Reaction of oxygen with the respiratory chain in cells and tissues. *J Gen Physiol* 1965;49:163–188.
- Hempel F, Jobsis F, LaManna J, Rosenthal M, Saltzman H. Oxidation of cerebral cytochrome aa3 by oxygen plus carbon dioxide at hyperbaric pressures. *J Appl Physiol* 1977;43:873–879.
- Erdmann W, Kunke S, Krell W. Tissue  $p\text{O}_2$  and cell function—an experimental study with multimicroelectrodes in the rat brain. In: Kesler M, Bruley D, Clark LC Jr, Lubbers D, Silver I, Strauss J, editors. Oxygen supply, theoretical and practical aspect of oxygen supply and microcirculation of tissue. Munchen-Berlin-Wien: Urban & Schwarzenberg 1973; p 167–174.
- Nair P, Whalen W, Buerk.  $\text{PO}_2$  of cat cortex: response to breathing  $\text{N}_2$  and 100%  $\text{O}_2$ . *Microvasc Res* 1975;9:158–165.
- Mitnick M, Jobsis F. Pyrenebutyric acid as an optical oxygen probe in the intact cerebral cortex. *J Appl Physiol* 1976;41:593–596.
- Jobsis F. Noninvasive infrared monitoring of cerebral and myocardial oxygen sufficiency and circulatory parameters. *Science* 1977;198:1264–1267.
- Liu KJ, Gast P, Moussavi M, Norby SW, Vahidi N, Walczak T, Wu M, Swartz HM. Lithium phthalocyanine: a probe for electron paramagnetic resonance oximetry in viable biological systems. *Proc Natl Acad Sci USA* 1993;90:5438–5442.
- Grieb P, Forster R, Strome D, Goodwin C, Pape P.  $\text{O}_2$  exchange between blood and brain tissues studied with  $^{18}\text{O}_2$  indicator-diffusion technique. *J Appl Physiol* 1985;58:1929–1941.
- Mason RP. Non-invasive physiology:  $^{19}\text{F}$  NMR of perfluorocarbons. *Artif Cells Blood Substit Immobil Biotechnol* 1994;22:1141–1153.
- Eidelberg D, Johnson G, Barnes D, Tofts PS, Delpy D, Plummer D, McDonald WI.  $^{19}\text{F}$  NMR imaging of blood oxygenation in the brain. *Magn Reson Med* 1988;6:344–352.
- Dardzinski BJ, Sotak CH. Rapid tissue oxygen tension mapping using  $^{19}\text{F}$  inversion recovery echo planar imaging of perfluoro-15-crown-5-ether. *Magn Reson Med* 1994;32:88–97.
- Holland SK, Kennan RP, Schaub MM, D'Angelo MJ, Gore JC. Imaging oxygen tension in liver and spleen by  $^{19}\text{F}$  NMR. *Magn Reson Med* 1993;29:446–458.
- Le D, Mason RP, Hunjan S, Constantinescu A, Barker BR, Antich PP. Regional tumor oxygen dynamics:  $^{19}\text{F}$  PBSR EPI of hexafluorobenzene. *Magn Reson Imaging* 1997;15:971–981.
- Hees PS, Sotak CH. Assessment of changes in murine tumor oxygenation in response to nicotinamide using  $^{19}\text{F}$  NMR relaxometry of a perfluorocarbon emulsion. *Magn Reson Med* 1993;29:303–310.
- Berkowitz BA, Wilson CA, Hatchell DL, London RE. Quantitative determination of the partial oxygen pressure in the vitrectomized rabbit eye in vivo using  $^{19}\text{F}$  NMR. *Magn Reson Med* 1991;21:233–241.
- Silva AC, Zhang W, Williams DS, Koretsky AP. Multi-slice MRI of rat brain perfusion during amphetamine stimulation using arterial spin labeling. *Magn Reson Med* 1995;33:209–214.
- Silva A, Lee S-P, Yang C, Iadecola C, Kim S-G. Simultaneous BOLD and perfusion functional MRI during forepaw stimulation in rats. *J Cereb Blood Flow Metab* 1999;19:871–879.
- Duong TQ, Silva AC, Lee S-P, Kim S-G. Functional MRI of calcium-dependent synaptic activity: cross correlation with CBF and BOLD measurements. *Magn Reson Med* 2000;43:338–392.
- Duong TQ, Kim S-G. In vivo MR measurements of regional arterial and venous blood volume fractions in intact rat brain. *Magn Reson Med* 2000;43:392–402.
- Duong TQ, Ackerman JJH, Ying HS, Neil JJ. Evaluation of extra- and intracellular apparent diffusion in normal and globally ischemic rat brain via  $^{19}\text{F}$  NMR. *Magn Reson Med* 1998;40:1–13.
- Kety SS, Schmidt CF. The effects of altered arterial tensions of carbon dioxide and oxygen on cerebral blood flow and cerebral oxygen consumption of normal young men. *J Clin Invest* 1948;27:484–491.
- Novack P, Shenkin H, Bortin L, Goluboff B, Soffe AM. The effects of carbon dioxide inhalation upon the cerebral blood flow and cerebral oxygen consumption in vascular disease. *J Clin Invest* 1953;32:696.
- Riess JG, Krafft MP. Advanced fluorocarbon-based systems for oxygen and drug delivery, and diagnosis. *Artif Cells Blood Substit Immobil Biotechnol* 1997;25:43–52.
- Lin W, Paczynski RP, Kuppusamy K, Hsu CY, Haacke EM. Quantitative measurements of regional cerebral blood volume using MRI in rats: effects of arterial carbon dioxide tension and mannitol. *Magn Reson Med* 1997;38:420–428.

26. Lassen N. Brain. In: Johnson P, editor. *Peripheral circulation*. New York: Wiley; 1978. p 337–358.
27. Reivich M. Arterial pCO<sub>2</sub> and cerebral hemodynamic. *Am J Physiol* 1964;206:25–35.
28. Bereczki D, Wei L, Otsuka T, Acuff V, Pettigrew K, Patlak C, Fenstermacher J. Hypoxia increases velocity of blood flow through parenchymal microvascular systems in rat brain. *J Cereb Blood Flow Metab* 1993;13:475–486.
29. Faraci FM, Heistad DD. Regulation of the cerebral circulation: role of endothelium and potassium channels. *Physiol Rev* 1998;78:53–97.
30. Francois-Dainville E, Buchweitz E. Effect of hypoxia on percent of arteriolar and capillary beds perfused in the rat brain. *J Appl Physiol* 1986;60:280–288.
31. van der Sanden BP, Heerschap A, Simonetti AW, Rijken PF, Peters HP, Stuben G, van der Kogel AJ. Characterization and validation of noninvasive oxygen tension measurements in human glioma xenografts by <sup>19</sup>F-MR relaxometry. *Int J Radiat Oncol Biol Phys* 1999;44:649–658.
32. Cater DB. The significance of oxygen tension measurements in tissues. In: Payne JP, Hill DW, editors. *A symposium on oxygen measurements in blood and tissues and their significance*. London: J & A Churchill; 1966.
33. Rasio E, Goresky CA. Capillary limitation of oxygen distribution in the isolated rete mirabile of the eel (*Anguilla anguilla*). *Circ Res* 1979;44:498–503.
34. Iadecola C. Regulation of the cerebral microcirculation during neural activity. *TINS* 1993;6:206–214.
35. Fox PT, Raichle ME, Mintun MA, Dence C. Nonoxidative glucose consumption during focal physiologic neural activity. *Science* 1988;241:462–464.
36. Roland PE, Erickson L, Stone-Elander S, Widen L. Does mental activity change the oxidative metabolism of the brain? *J Neurosci* 1987;7:2373.
37. Kim S-G. Quantification of relative cerebral blood flow change by flow-sensitive alternating inversion recovery (FAIR) technique: application to functional mapping. *Magn Reson Med* 1995;34:293–301.
38. Moulder JE, Rockwell S. Hypoxic fractions of solid tumors: experimental techniques, methods of analysis, and a survey of existing data. *Int J Radiat Oncol Biol Phys* 1984;10:695–712.
39. Shockley RP, LaManna JC. Determination of rat cortical blood volume changes by capillary mean transit time analysis during hypoxia, hypercapnia and hyperventilation. *Brain Res* 1988;454:170–178.
40. Iwamoto J, Curran-Everett DC, Krasney E, Krasney JA. Cerebral metabolic and pressure-flow responses during sustained hypoxia in awake sheep. *J Appl Physiol* 1991;71:1447–1453.